JOURNAL OF AIRCRAFT
Vol. 31, No. 5, Sept.-Oct. 1994

Development and Flight Test of a Deployable Precision Landing System

Alex G. Sim,* James E. Murray,† and David C. Neufeld*
NASA Dryden Flight Research Facility, Edwards, California 93534
and
R. Dale Reed‡
PRC Inc., Edwards, California 93534

A joint NASA Dryden Flight Research Facility and Johnson Space Center program was conducted to determine the feasibility of the autonomous recovery of a spacecraft using a ram-air parafoil system for the final stages of entry from space that included a precision landing. The feasibility of this system was studied using a flight model of a spacecraft in the generic shape of a flattened biconic that weighed approximately 150 lb and was flown under a commercially available, ram-air parachute. Key elements of the vehicle included the Global Positioning System guidance for navigation, flight control computer, ultrasonic sensing for terminal altitude, electronic compass, and onboard data recording. A flight test program was used to develop and refine the vehicle. This vehicle completed an autonomous flight from an altitude of 10,000 ft and a lateral offset of 1.7 miles that resulted in a precision flare and landing into the wind at a predetermined location. At times, the autonomous flight was conducted in the presence of winds approximately equal to vehicle airspeed. Several novel techniques for computing the winds postflight were evaluated. Future program objectives are also presented.

Introduction

NASA is studying a variety of vehicles for use in returning humans and cargo from space to Earth. Although the configuration of these vehicles is not yet confirmed, several capsule shapes are under consideration. Hinson[1] proposes the use of the Assured Crew Return Vehicle as a "lifeboat" for Space Station Freedom and is studying land and water options using parachutes and a touchdown attenuation system. The Personnel Launch System will return crew members and biological experiments from low Earth orbit. Any other mission using a capsule vehicle could benefit from the use of a deployable, precision, autonomous landing system.

The use of deployable, ram-air-inflated, gliding parachutes for spacecraft recovery has been proposed since the mid 1960s.[2,3] Studies for the Gemini and Apollo programs included the use of parasails, sailwings, and Rogallo parawings for spacecraft recovery. The primary problems with these systems involved inflation performance and reliability. Although performance of these systems was promising, lack of an extensive experience base hurt their chances for use in a large-scale recovery program. Inability to control the high horizontal velocities developed during flight also made these systems unacceptable.

The emergence of the ram-air-inflated parafoil as the parachute of choice among sport jumpers has brought the issue of using gliding parachutes for spacecraft recovery back into the forefront of this area of research. Reliability issues that raised concerns during the 1960s have been reduced because of the high number of systems in sport use today and the advancements in technology.[4,5] The Advanced Recovery Systems Program focused on developing a large-scale gliding recovery system.[6] Although canceled after nine flight tests, this program was successful in developing a unique inflation loads management system for large parafoils.

Potential NASA users for this technology include the manned space programs listed above as well as such unmanned vehicles as planetary probes and booster recovery systems. Other potential users include the U.S. Navy, which is studying the use of autonomous gliding parachute systems on aircraft ejection seats, and the U.S. Army and Air Force. These latter potential users prefer high-altitude, offset delivery of cargo to minimize danger to aircraft and crews.

To develop a deployable precision landing system, NASA Dryden Flight Research Facility, Edwards, California, and Johnson Space Center, Houston, Texas, are participating in a joint program called the Spacecraft Autoland Project. The phase 1 program goals were to air-drop a vehicle from an altitude of 10,000 ft, deploy a parafoil, fly autonomously using Global Positioning System (GPS)[7] navigation to a predetermined landing site; fly a descending pattern over the site until reaching a specified altitude, and fly downwind, turn onto final approach into the wind, flare, and land within one-fourth mile of the predetermined site. A generic spacecraft shape, the flattened biconic (Spacewedge), was chosen as the flight vehicle. A custom harness was adapted between the vehicle and a ram-air parachute. The vehicle contained a radio uplink, servoactuators, flight control computer, and GPS receiver. Off-the-shelf equipment was used whenever possible in this project to keep costs low and to reduce development time.

This report summarizes the results of phase 1 of the Spacecraft Autoland Project. The vehicle, design, and control concepts are described. Steps leading toward the final flight demonstration are detailed. The flight results, the lessons learned, and a sample of flight data are given. In addition, the results of a novel postflight study that used data from the flights to compute wind velocities using two estimation techniques are shown. Future phase 2 objectives are also presented.

Received July 1, 1993; revision received Oct. 7, 1993; accepted for publication Jan. 9, 1994; presented as Paper 94-2141 at the 7th Biennial AIAA Flight Test Conference, June 20–23, 1994. Colorado Springs, CO.

*Aerospace Engineer, M/S D-2033.
†Aerospace Engineering Technician, M/S D-4820-1D.
‡Senior Aerospace Engineer, M/S D-4839-B.

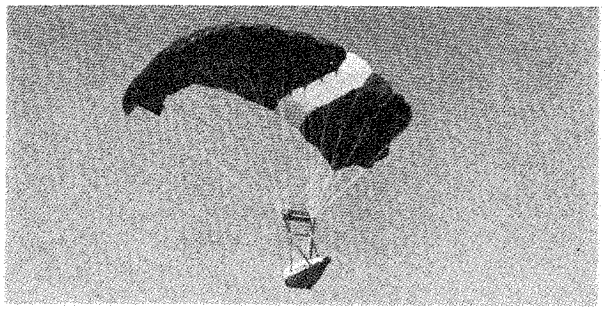

Fig. 1 Spacewedge vehicle.

Vehicle Description

The Spacewedge consisted of the flattened biconic airframe that was joined to a ram-air parafoil with a custom harness. In the manual control mode, the vehicle was flown using a radio uplink. In the autonomous mode, the vehicle was controlled using a small computer that received inputs from onboard sensors. Selected sensor data were recorded onto several onboard data loggers.

Airframe

Figure 1 shows the Spacewedge. This vehicle is roughly 4 ft long and weighs 150 lb. Table 1 provides a detailed list of the physical characteristics. A flattened biconic was chosen as a representative hypersonic shape for the vehicle, although the aerodynamics of any representative hypersonic shape will have only minor effects on the flying qualities while under a parafoil. The primary structure of this vehicle was tubular steel because of the need for it to withstand hard landings. This structure was covered with plywood on the bottom and rear skins, had a wooden nose, and had removable aluminum upper and side skins. Where possible, vehicle costs, cosmetics, and complexities were limited because a few hard landings were expected. In addition, the project benefited from keeping the value of the vehicle low because this approach tends to diminish the need for system redundancy.

Parafoil

The parafoil chosen for the phase 1 tasks was a ram-air parachute of 288 ft^2 (Table 1). Such parachutes are commonly used for initial student flight instruction. The docile flight characteristics, low wing loading (near 0.5 lb/ft^2), and proven design allowed the project team to concentrate on developing the vehicle rather than the parachute. As an example of the added safety with the large parachute, bringing the vehicle down without landing flare and without sustaining damage was possible. The flare maneuver required control line pull of 40 in. with a peak of approximately 20 lb of force. In parafoil terminology, "full brake" refers to the condition of fully contracted (pulled) control lines and results in vehicle flare, whereas "full flight" refers to fully extended control lines and results in high-speed flight. With the exception of lengthened control lines, the parachute rigging was not modified. Lengthened control lines were attached to servodrums. A fabric-sliding device, which is traditionally used to soften the opening loads of ram-air parachutes, called a square slider, was retained on this chute (Fig. 2). The project concept was to substitute a smaller parachute once the vehicle was developed. This small parachute would allow for a wing loading more representative of a space vehicle application (near 2 lb/ft^2).

Harness

The harness was designed for stability with front and rear attachment points on each side of the vehicle (Fig. 2). Each side of the harness then triangulated to a common location analogous to a parachutist's shoulder point. A nylon web was used to separate these shoulder points. A static line was used for parachute deployment. After deployment, a full brake input (pull down) was used to release the control line.

Table 1 Physical characteristics

Vehicle	
Length, vehicle only	45.3 in.
Length, with packed parachute	53.0 in.
Height	21.7 in.
Span	31.5 in.
Nose radius	1.8 in.
Total cone angle, forebody	36 deg
Total cone angle, aft body	33 deg
Base area	515 in.^{2}
Weight	150 lb
Parachute	
Span	27.5 ft
Chord	10.5 ft
Area	288 ft^2
No. of cells	9
Aspect ratio	2.62
Pack volume	627 in.^{3}
Weight	11 lb

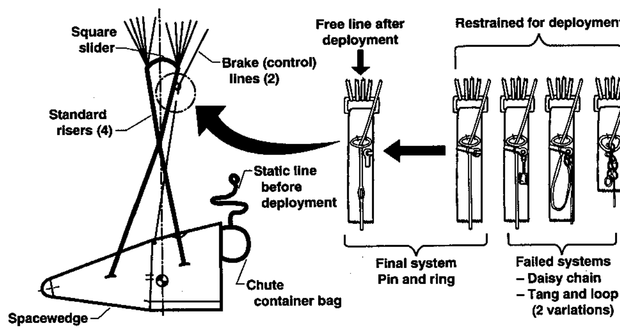

Fig. 2 Brake line deployment restraint development.

Considerable harness development effort centered on protecting the control servoactuators from the opening shock loads of the parachute while allowing a commanded clean release of the control lines. To accomplish this goal, harness designs using daisy chain and tang-and-loop techniques were investigated (Fig. 2). Both techniques either did not always release the control line or caused the line to jam after release. The final pin-and-ring configuration provided a positive release and did not tend to jam the line (Fig. 2).

Vehicle Details

The architecture of this instrumentation system was driven by cost, hardware availability, and program evolution. Figure 3 shows a cutaway sketch of the Spacewedge vehicle. Figure 4 shows both the essential items for the phase 1 task and the items that were added for instrumentation purposes. These essential items consisted of the uplink receiver, GPS receiver and antenna, barometric altimeter, flight control computer, servoactuators, electronic compass, and ultrasonic altimeter. Added instrumentation included a video camera, a video 8-mm camcorder, the control position transducers for measuring control line position, a data logger, and a pocket personal computer. Many of the control system hardware components and related software were commercially obtained. The uplink, servoactuators, instrumentation, and accompanying systems were integrated by NASA employees.

The GPS is a navigation system based on position information from a constellation of satellites. The GPS hardware used was a commercially available, 5-channel, coarse acquisition (C/A) code receiver without differential GPS (DGPS) capability. When selective availability (SA) is activated, a slow, random error is superimposed on the position solution characteristic of C/A code.

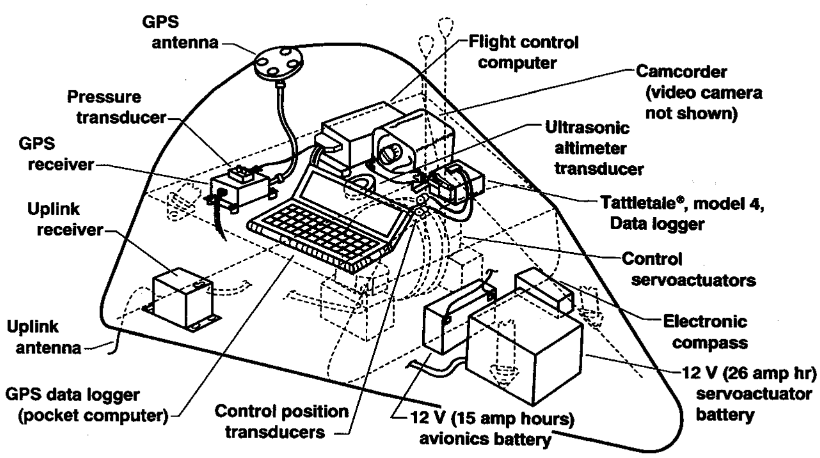

Fig. 3 Cutaway drawing of Spacewedge vehicle.

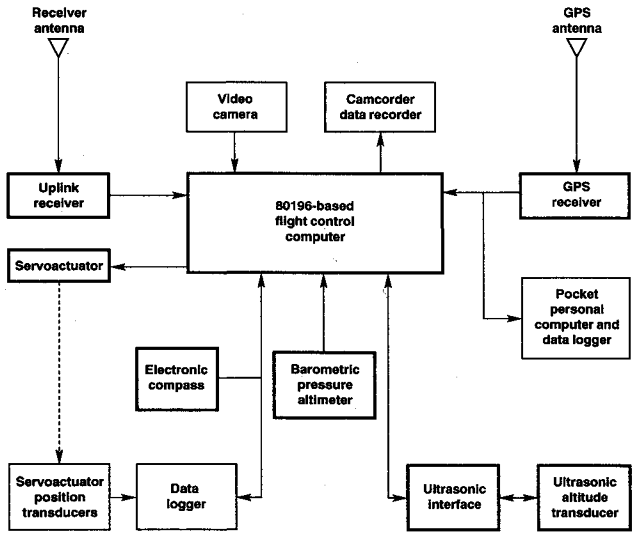

Fig. 4 Phase 1 avionics.

Figure 4 also shows the instrumentation system that consisted of a video system and two digital data loggers. This system used a camera to provide a carrier signal with frame synchronization. The flight control computer overlaid graphical and character data onto the carrier signal which was then recorded in the camcorder. Video data consisted of information pages generated from the flight control computer. These pages were updated 10 times/s and included GPS coordinates and computed velocities, control commands, magnetic compass heading, pressure altimeter, ultrasonic altimeter, and various status indicators. The pocket personal computer[8] was used as a data logger to digitally record the GPS coordinates. An additional data logger[9] was used to digitally record control surface positions and magnetic compass headings. Data from both data loggers were downloaded into a ground-based computer for postflight analysis.

Control Modes

The control system had programming, manual flight, and autonomous flight modes. The programming mode was used to initialize and configure the flight control computer. Landing coordinates were captured by placing the vehicle into the programming mode while at the landing site. Decision altitudes, the altitudes where the flight control computer changed logic, and ground wind velocity could be programmed through the uplink transmitter controls while the programming page was being viewed on the video camcorder.

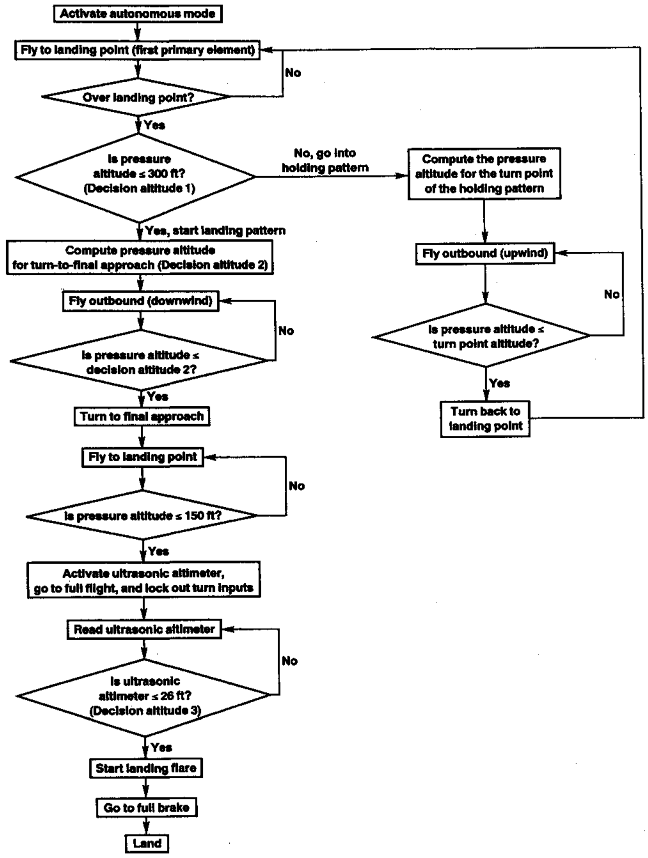

Fig. 5 Conceptual autonomous mode logic.

The manual mode used a radio control (RC) model receiver and uplink transmitter. The uplink signal was boosted to 15 W, and a government-authorized frequency was used. The transmitter was configured to allow the ground pilot to enter either brake (pitch) or turn (yaw) commands. The vehicle reverted to manual mode whenever the transmitter controls were moved, even when the autonomous mode was selected. In the manual mode, the transmitter commands passed through—but were not altered by—the flight control computer.

Figure 5 shows the conceptual logic diagram for the autonomous mode. Flight in this mode included four primary elements and three decision altitudes. The four elements were 1) navigate to the landing point, 2) maintain the holding pattern while descending, 3) enter the landing pattern, and 4)

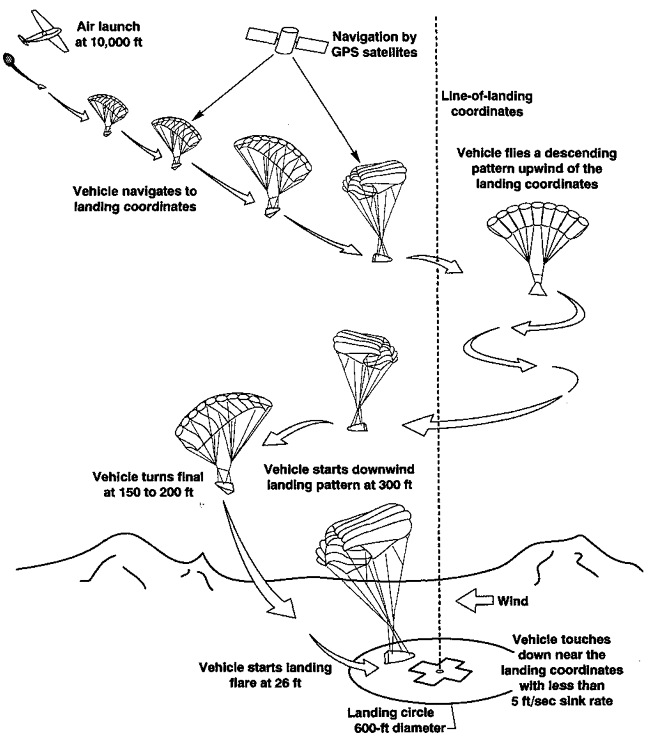

Fig. 6 Autonomous mode control elements.

initiate the flare maneuver (Fig. 6). The three decision altitudes were at the 1) start of the landing pattern, 2) turn to final approach, and 3) flare initiation.

When at high altitude and offset from the landing point, the vehicle was commanded to fly to the landing point. If the landing point was reached while at or above the first decision altitude (typically set to 300 ft), then the vehicle was commanded to fly a holding pattern until it descended below the decision altitude. The holding pattern was an upwind racetrack pattern aligned with the wind (as input in the programming mode) and made of outbound (upwind) and inbound (downwind) legs. Each lap of the racetrack pattern consumed approximately 500 ft of altitude. Wind velocity was an input to the flight control computer. Below the first decision altitude, the vehicle was commanded to enter the landing pattern, which consisted of a downwind leg and a 180-deg turn to final approach.

The point to turn to final approach was based on a second decision altitude, typically 150–200 ft. This second altitude was a function of the wind (as input in the programming mode) and the position relative to the landing point. Once on final approach, the vehicle was commanded to full flight (maximum speed), steering commands were locked out, and the ultrasonic altitude sensor was activated.

At a third and final decision altitude (typically 26 ft as measured using the ultrasonic altimeter), the flare was initiated by commanding full brake. Touchdown occurred 3.5–4 s later.

Flight Operations

The steps toward the final demonstration included developing the harness, refining the control system, and conducting several ground tests. A second inert Spacewedge vehicle was used to validate parachute deployment and drop-separation characteristics. Both Spacewedge vehicles were launched (dropped) from light and from remotely piloted aircraft. The flare maneuver was constrained by servoactuator characteristics. Two wind estimation techniques were also investigated.

Many interim steps were taken to reach the final demonstration of autonomous flight. This section highlights selected flights. From flights 1–9, the Spacewedge was remotely controlled with only the uplink receiver and the control servoactuators installed. The autonomous system was first installed for flight 9, but was only used as a source of data (recorded on video) until flight 18. Starting with flight 18, the autonomous control mode was often engaged and evaluated. The final control algorithms were implemented starting with flight 29. The final flight demonstrations occurred on flights 33–36.

Flights 1 and 2 were to slope soar the Spacewedge from a hillside with approximately 15 kt of wind. These flights were used to evaluate general flying, including gentle turns and landing flare, and servoactuator capabilities. The first flight was never more than 10 ft above the slope. The second flight achieved an altitude of approximately 50 ft.

Initially, to validate parachute deployment, harness design, and drop-separation characteristics, a second Spacewedge vehicle was fabricated with the same external geometry and weight as the first vehicle. This second vehicle (inert Spacewedge) was inexpensive, without internal components, and considered expendable. This vehicle was launched from the light aircraft, flights 3 and 4, and yielded significant confidence in the success of parachute deployment before the first drop of the more valued primary Spacewedge vehicle. During flight 9, the inert Spacewedge was also first launched from an ultralight airplane before the launch of the primary Spacewedge from this airplane during flight 12. Flights 9 and 12 were the only two flights in which this ultralight airplane was used.

Through flight 17, refinements were made to the harness as well as to the estimates of the turn-control authority. Estimates of the time and altitude required to flare were also refined. Before the Spacewedge could be considered reliable, it was necessary to develop the pin-loop-ring that was used to protect the control servoactuators from the opening shock loads. While the harness development continued, the autonomous electronics were installed, and their performance was passively monitored. During flights 15 and 16, turn-control authority data were obtained by recording the time to turn resulting from step-commanded inputs. Figure 7 shows the control power as measured during these flights. The uncertainty of the actual servoactuator position forced the installation of control position transducers and started the process of adding digital data loggers onboard the vehicle. Estimates were also made of the time and altitude required to flare.

Once the autonomous system was installed, several ground tests were conducted. One test used to roughly validate the steering commands involved carrying the Spacewedge and an observer out onto a dry lakebed in the back of a pickup truck. After acquiring lakebed landing site coordinates into computer memory, the truck would be driven a few thousand feet away at roughly the 20-mph flight speed of the Spacewedge. The observer would then translate Spacewedge servoactuator position into left- or right-turn instructions for the truck driver. This test proved effective as a means of getting a crude zero-wind simulation of the functioning of the GPS receiver and flight control computer.

A second ground test involved a crane to check the functionality of an ultrasonic altimeter that was used to determine ground height for landing flare initiation. The original Spacewedge concept involved downlinking the control computer data display to a ground-based video monitor; however, the video downlink degraded the ultrasonic range of the altimeter from 35 ft down to approximately 20 ft. Because a range of

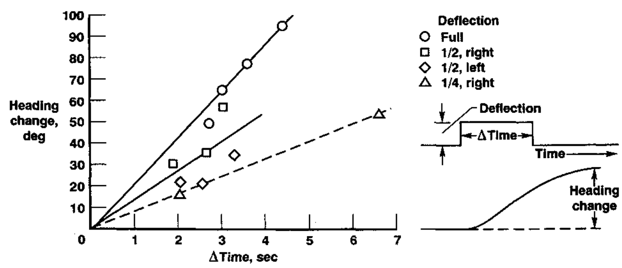

Fig. 7 Control power as measured from flights 15 and 16.

approximately 30 ft was needed, many variations in transmitter and antenna location were evaluated by hoisting the Spacewedge up to 35 ft under a crane. After achieving limited success with this test, the team decided to record the video signal onboard. Whenever the electrical configuration was changed, the crane was used to verify the accuracy of the ultrasonic altimeter sensing.

The autonomous flight mode could be selected from the uplink transmitter. The vehicle would typically be left in autonomous mode until this mode failed to perform as desired. Problems with the control logic were common during the early autonomous mode flights because many control algorithms were evaluated. The team considered the ability to immediately revert to manual mode mandatory. While in autonomous mode, the turn performance, navigation, and automatic flare of the vehicle were evaluated. Decision heights and turn-performance parameters were often adjusted between flights.

Launch Vehicles

The Spacewedge was usually carried to the test altitude in a light airplane (Fig. 8). At a designated landing area, it was pushed out the side of the airplane with a 15-ft static line attached. Initially, the Spacewedge faced aft of the flight direction of the airplane. No problems were encountered with parachute dynamics or loads.

Early in the project, an ultralight airplane was modified for use as a remotely piloted, slow-speed, launch vehicle (Fig. 9). Both the primary and the second inert Spacewedge vehicles were dropped from this ultralight airplane. On the one hand, use of this airplane had the added advantage of launching these vehicles straight ahead with an 8-ft static line to minimize opening shock loads. On the other hand, this approach proved to be significantly more complex and labor intensive than using the light airplane. Once the light aircraft (Fig. 8) proved its viability, the ultralight airplane was no longer used.

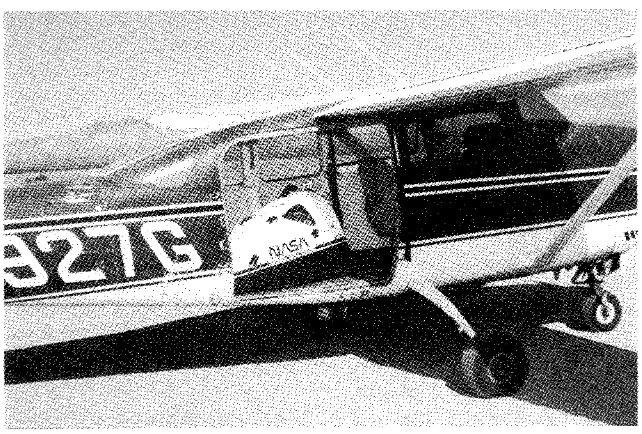

Fig. 8 Spacewedge inside of the light airplane launch aircraft.

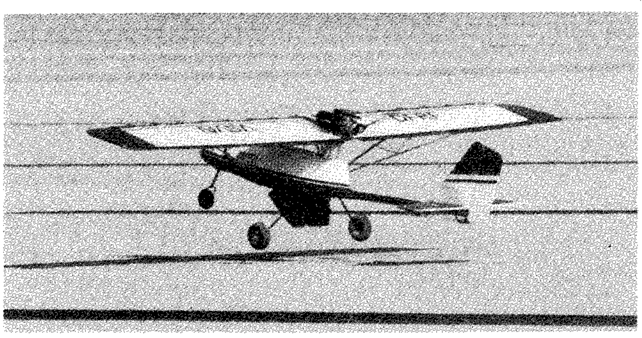

Fig. 9 Spacewedge attached to the ultralight remotely piloted airplane.

Typical Flights

After completing the initial checklists and then loading and unloading the support vehicles, the first key element of a typical flight operation was to place the Spacewedge in the target area for initialization of the programming mode of the flight control computer. At the target area, landing coordinates, ground windspeed, wind direction, and decision altitudes were stored into the memory of this computer. Then the Spacewedge was transported to the launch airplane. Once good GPS reception (lock) was ascertained, the Spacewedge was loaded into the launch airplane. Because maintaining good reception was impossible inside the launch vehicle, the GPS lock would be lost for as long as 15 min. The lock could not be reacquired until approximately 40 s after launch.

After a successful launch and a good parachute opening had been verified, manually commanding full brake (pull down) to release the control lines was necessary. Left and right turns were then commanded to verify free controls and to check the general functionality of the uplink. Approximately 1 min after launch, the autonomous mode was engaged. Then the Spacewedge flew toward the landing coordinates. At that time, the logic changed and a descending holding pattern was established with its major axis aligned with the wind direction. This pattern continued until the vehicle reached a decision altitude of typically 300 ft where it started a downwind leg. At altitudes between 150–200 ft, the vehicle turned into an upwind final leg. At a nominal altitude of 26 ft as determined by the ultrasonic altimeter, full brake was commanded and flare was initiated. Approximately 3.5–4 s later, the vehicle landed.

Flare Technique

A technique similar to one that sport parachutists have perfected through decades of trial and error was considered for use as the initial landing flare for the Spacewedge. The parachutist initiates landing flare at an altitude of roughly 5–7 ft above the ground and completes the flare in approximately 1 s. The Spacewedge initiates flare at an altitude of 26 ft and requires approximately 3.5 s to complete the flare. To emulate a parachutist, the 40 in. of control line travel required for full brake (flare) would have to be pulled in 1 s. To stay within the power available from the electric servoactuators, a 10-in.-diam drum was used to reel the control lines of the Spacewedge. To achieve the required line travel with flight loads, the servoactuators required approximately 3.5 s to achieve full brake. Thus, a flare initiation altitude of approximately 26 ft above the ground was needed to allow 3.5 s to touchdown. The landing flare technique was dictated by slow servoactuator speed and, in essence, limited to the open-loop task of when to initiate flare. Without control feedback to compensate for wind or terrain variations, landings averaged a sink rate of 2 ft/s. Note that the navigation task can be accomplished with relatively slow servoactuators of limited travel; whereas, the flare maneuver required relatively large servoactuators.

Wind Estimation Maneuvers

During phase 1, horizontal wind estimates were not computed as part of the navigation task. On the other hand, flight test data recorded onboard during the flight allowed postflight wind estimates to be computed. Two estimation techniques were tried, and one was compared with an independent wind measurement.

The first technique required manually holding the Spacewedge in a steady turn for approximately three circles. Without wind, the ground track from this three-circle maneuver would be three overlaid circles. With wind, the Spacewedge drifted downwind while executing the circles. The resulting ground track is the superposition of the circles (motion of the Spacewedge in the air mass) and the wind drift (motion of the air mass with respect to the ground). A mathematical model of the ground track was constructed. The model assumed a steady turn and a constant wind. A least-squares estimation technique was used to compute such model parameter values as wind components, turn radius, and turn rate. These parameters gave the best fit to the recorded GPS data for the maneuver. As an advantage, this technique also estimates vehicle airspeed and, thereby, alleviates the need to directly measure airspeed. This technique is appropriate for research maneuvers but not for real-time computation of winds.

The second technique used the conventional approach of vectorially subtracting airspeed from ground speed to yield windspeed.[10] Airspeed was not measured but assumed to be 30 ft/s (the measured average using the first technique). The direction of the airspeed was measured with the onboard electronic compass, and the angle of sideslip was assumed to be zero. Ground speed was measured with the GPS. As expected, unmeasured motion of the Spacewedge during maneuvering flight made most of the wind measurements very noisy; only data from straight, steady-flight conditions were usable. Although this conventional technique requires a vehicle airspeed measurement, it is a reasonable technique to use for real-time wind computation. Using this second technique, logic and filtering will need to be used to reduce the noise.

Phase 1 Flight Results

The effects of even moderate winds on a slow-flying vehicle drove the development of the navigation algorithms and dictated the use of a compass. Winds were estimated postflight using data from GPS and the compass and are compared with radar data. Results of the flight testing included lessons learned, flight demonstrations, autolanding and postflight evaluations of two techniques for computing wind data. The following subsections provide a detailed discussion of these results.

Lessons Learned

Because of the SA imposed on the signals received by commercially available GPS receivers, errors in the two-dimensional-position solution as large as 600 ft were observed in a 15-min period. The effect of SA on the navigation task was a random bias of the landing point of the vehicle during the autonomously navigated flights. This effect on the navigation error could be largely eliminated by using either a precision code receiver (P code, used by the military) or by using equipment with DGPS capability. On the other hand, both of these solutions required more complicated and expensive systems than were considered necessary for phase 1.

Before flight 29, only GPS position and velocity measurements were used in the navigation algorithms. This usage worked well with relatively calm winds. With even moderate 10- to 15-mph winds, however, these simple algorithms failed in some cases. These failures became complete as the winds approached and exceeded the 20-mph flight speed. While onboard, real-time wind estimation would allow use of a more robust navigation algorithm. This use was beyond the scope of phase 1. A simpler solution was to use GPS to establish target coordinates and to use an electronic compass to determine heading corrections to those coordinates. This solution eliminated the need for onboard wind estimation, but yielded a less precise flight pattern.

Flight Demonstrations

Two autonomous demonstration flights were made: one from an altitude of 6000 ft and another from 10,000 ft. Figure 10 shows the ground track for flight 33. This flight from an altitude of 6000 ft was flown with relatively calm winds and typically illustrates the elements of the pattern.

Figures 11a and 11b show the ground track of flight 34. These data show the GPS ground track of the vehicle that was dropped from an altitude of approximately 10,000 ft with an approximately 1.7-mile lateral offset from the target and with significant winds. At these high altitudes, the windspeed

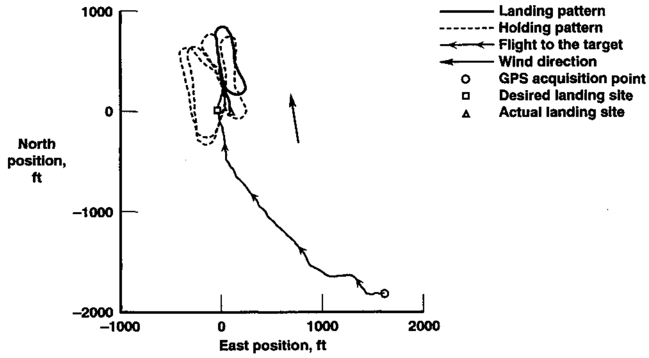

Fig. 10 Ground track of flight 33 from an altitude of 6000 ft.

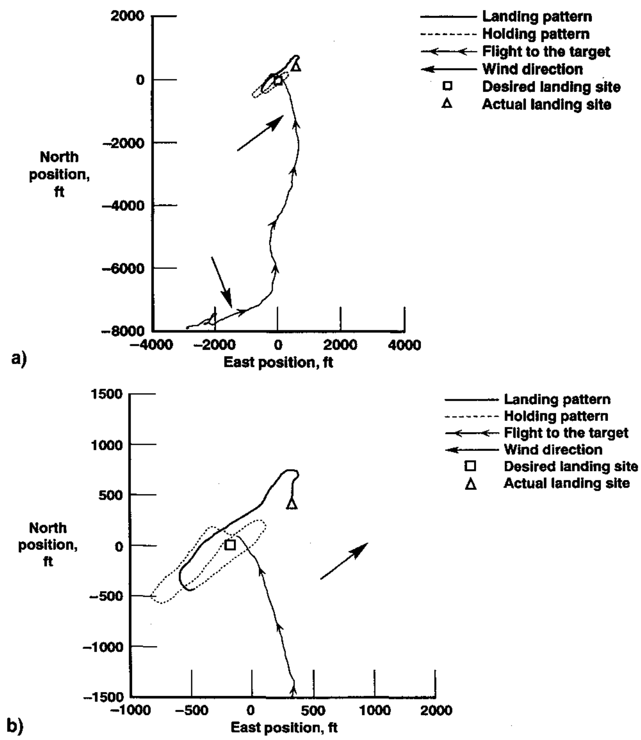

Fig. 11 Ground track of flight 34 launched from an altitude of 10,000 ft: a) complete flight and b) terminal area.

was approximately the same magnitude as the forward speed of the Spacewedge. As a result, the Spacewedge was blown to the southwest of the landing coordinates and was unable to penetrate the wind and progress toward the landing coordinates until it was below an altitude of 6000 ft. The flight to the landing point, the holding pattern, and the landing pattern are highlighted in these figures and, again, shown to work well. Flights 35 and 36 were partial demonstration flights with the final one-half of each flight in the autonomous mode. For flights 33–36, the average touchdown distance from the target was approximately 400 ft.

Autolanding

Landing in autonomous mode is best illustrated by the ultrasonic altimeter time history (Fig. 12). For this landing, flare was initiated at 26 ft with a sink rate of nearly 10 ft/s. At touchdown, the sink rate was reduced to below 2 ft/s. On this landing, excellent results were obtained using simple control logic. Figure 13 gives an example of the control line travel during landing flare. The corresponding faired ultrasonic altitude time history is also given. At touchdown, the sink rate for this flight was approximately 2.5 ft/s.

Postflight Wind Estimates

On the last flight of phase 1, flight 36, two three-circle maneuvers were manually performed while at an altitude above

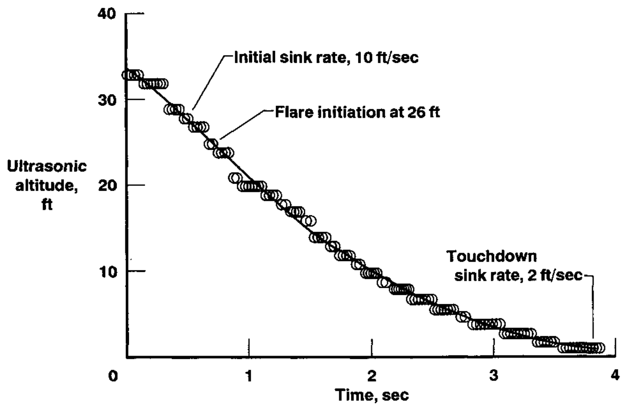

Fig. 12 Landing flare for flight 28.

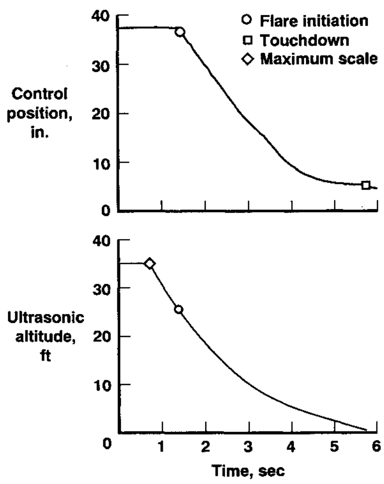

Fig. 13 Landing flare control surface position and ultrasonic altitude for flight 35.

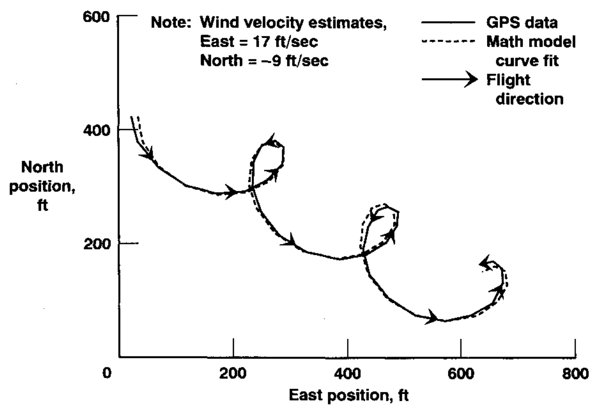

Fig. 14 Three-circle maneuver as measured using the Global Positioning System and computed for flight 36.

6000 ft. Figure 14 shows the GPS-measured ground track of one maneuver with the ground track computed from the mathematical model overlaid. This maneuver yielded E and N wind components of 17 and −9 ft/s, respectively, and an airspeed estimate of 31 ft/s. Figure 15 shows the wind estimates plotted along with the radar measurements from these two maneuvers. Each maneuver spanned an altitude of several hundred feet. The analysis assumed constant wind over this range of altitudes.

Ten minutes before flight 36, foil-covered streamers were released from the launch aircraft over the target area and were tracked by the NASA Fixed Position System (FPS) 16 radar,[11] located 14 miles away. Comparisons between the radar measurements and computed winds showed good agreement to within approximately 2 ft/s, even though the assumption of constant wind during the maneuver was violated.

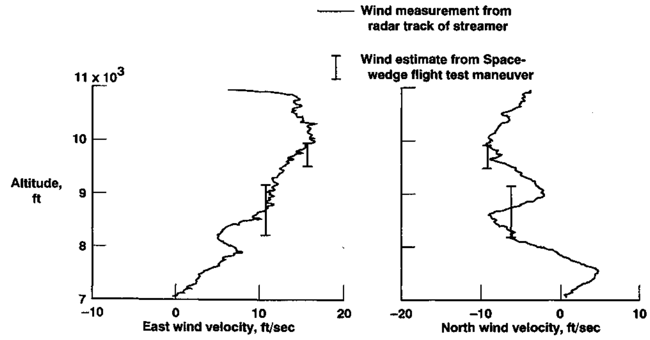

Fig. 15 Comparison of the three-circle maneuver results with the radar data.

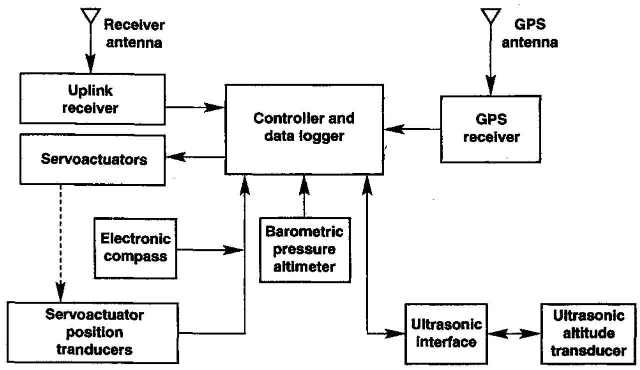

Fig. 16 Phase 2 avionics.

The second wind estimation technique was previously validated to be a good real-time estimator.[10] Thus, having independent radar data to correlate with these flight measurements was considered unnecessary. Data computed using the second technique appeared reasonable.

Phase 2 Objectives

In phase 1, an example of a precision deployable landing system for a model spacecraft was developed and autonomously flown from an altitude of 10,000 ft. The effort focused on the feasibility of the concept through flight demonstration. The concept of a flexible deployable system that uses autonomous navigation and landing was proved to be a viable and practical technique to use in recovering spacecraft. To focus the phase 1 scope, the approach to flight demonstration chose to use acceptable, commercially available, vehicle elements. Examples of these engineering compromises were to use a conservatively large parachute and slow servoactuators. Phase 2 is slated to investigate these compromises and to continue development of specific elements of phase 1.

Full-scale space vehicles are envisioned to fly under parafoils with wing loadings near 2 lb/ft^2. The vehicle flown in phase 1 had a wing loading near 0.5 lb/ft^2. Increasing the wing loading by a factor of 4 doubles the flying speed. The landing task is more complex than the navigation task although the latter remains relatively unchanged. With a wing loading of 2 lb/ft,^{2} the vehicle has the energy to perform a more precise flare maneuver and to balloon or climb during the flare. As a high-priority objective, phase 2 will investigate landing flare techniques with a small, commercially available, ram-air parachute of 88 ft^2. The flight demonstration task remains relatively unchanged. Exhibiting serendipity, the smaller chute has less demanding servoactuator requirements because of lower control line forces (approximately 10 lb) and less control line travel requirements (approximately 15 in.).

To accomplish phase 2, the flight algorithms used in phase 1 will be upgraded. With the addition of an airspeed sensor, it will be possible to compute windspeeds using the currently available GPS data, barometric altimeter, and compass system. With onboard wind data, much more nearly precise navigation will be possible. The program will be conducted using a combination flight control computer and data logger. NASA personnel will integrate the hardware with an architecture similar to that shown in Fig. 16.

The servoactuators used in phase 1 had approximately 14 of torque with a speed of 1 revolution every 2 s. Although impressive, these servoactuators marginally accomplished the phase 1 flare maneuver. When scaled up to a full-sized space vehicle, their size, weight, and power requirements become unattractive. This unattractiveness is true even with increased wing loading. Because only small servoactuators are needed for the navigation task, continued use of servoactuators for turn (yaw) control is reasonable. On the other hand, completing the flare maneuver without using servoactuators is desirable. Thus as a second objective, phase 2 will investigate alternate landing flare techniques. Developing the ability to use a stored energy device for flare actuation will be the key task in reaching this objective. Other techniques to be investigated as resources permit include gravity flare (a mass is shifted to pull the control lines) or rapid extensions of the chute leading-edge risers to produce nearly instantaneous lift and drag increments.

Concluding Remarks

A joint NASA Dryden Flight Research Facility and Johnson Space Center program was conducted to determine the feasibility of the autonomous recovery of a spacecraft using a ram-air parafoil system for the final stages of entry from space. The feasibility was studied using a flight model of a spacecraft with a generic flattened biconic shape that weighed approximately 150 lb and was flown under a ram-air parachute. Key elements of the vehicle included Global Positioning System guidance for the autonomous navigation, a flight control computer, an electronic compass, the ultrasonic sensing for terminal altitude, and the onboard data recording. A flight test program was used to develop and refine the vehicle. Development included several ground tests and manual flight using a radio uplink. The vehicle demonstrated autonomous flight in the presence of winds roughly equal to the vehicle airspeed from an altitude of 10,000 ft and a lateral offset of 1.7 miles. This demonstration resulted in a precision flare and landing into the wind at a predetermined location. Several techniques for computing wind components were investigated. The concept of a flexible deployable system that uses autonomous navigation and landing proved to be a viable and practical technique for recovering spacecraft.

References

[1]Hinson, J. K., "Application of Gliding Parachutes to the Space Station Crew Emergency Return Vehicle," Johnson Space Center (NASA) JSC-22820, Dec. 1987.

[2]Naoseth, R. L., "An Exploratory Study of a Parawing as a High-Lift Device for Aircraft," NASA TN D-629, Nov. 1960.

[3]Libby, C. E., and Johnson, J. L., Jr., "Stalling and Tumbling of a Radio-Controlled Parawing Airplane Model," NASA TN D-2291, July 1964.

[4]Knacke, T. W., "Parachute Recovery Systems Design Manual," NWC TP-6575, March 1992.

[5]Maydew, R. C., Peterson, C. W., and Orlik-Rucckemann, K. J., "Design and Testing of High-Performance Parachutes," AGARD-AG-319, Nov. 1991.

[6]Wailes, W. K., "Advanced Recovery Systems for Advanced Launch Vehicles (ARS) Phase 1 Study Results," AIAA Paper 89-0881, April 1989.

[7]*Global Positioning System*, Vols. 1–3, Inst. of Navigation, Washington, D.C., 1980–1986.

[8]*ZEOS Pocket PC User's Manual*, Zeos International, Ltd., Minneapolis, MN.

[9]Hamory, P. J., and Murray, J. E., "Flight Experience with Lightweight, Low-Power Miniaturized Instrumentation Systems," AIAA Paper 92-4111, Aug. 1992; see also NASA TM-4463, March 1993.

[10]Bjarke, L. J., and Ehernberger, L. J., "An In-Flight Technique for Wind Measurement in Support of the Space Shuttle Program," NASA TM-4154, Nov. 1989.

[11]Anderson, K. F., Wrin, J. W., and James, R., "A Radar Data Processing and Enhancement System," NASA TM-88274, Aug. 1986.